International Journal of Cardiology 461 (2026) 134670

Contents lists available at ScienceDirect

International Journal of Cardiology

journal homepage: www.elsevier.com/locate/ijcard

Septal thickness to QRS voltage ratio in Lead I/aVR: A simple tool for estimating cardiac amyloid burden

Matteo Sclafani [a,b,*], Luca Arcari [c], Giacomo Tini [a], Damiano Venturiello [a], Andrea Imperatrice [a], Alessandro Tropea [a], Elisa Fedele [d], Fabiana Romeo [d], Annamaria Martino [d], Domitilla Russo [e], Armando Fusco [f], Pietro Francia [a], Giovanni Camastra [c], Elisa Silvetti [d], Stefano Canestrelli [d], Leonardo Calò [d], Luca Cacciotti [c], Chiara Lanzillo [d], Francesco Cappelli [g], Beatrice Musumeci [a,1], Emanuele Barbato [a,1]

[a] Cardiology Unit, Department of Clinical and Molecular Medicine, Sant'Andrea University Hospital, Sapienza University, Rome, Italy
[b] Royal Brompton Hospital, London, UK
[c] Cardiology Unit, Madre Giuseppina Vannini Hospital, Rome, Italy
[d] Cardiology Unit, Policlinico Casilino, Rome, Italy
[e] Cardiology Unit, Ospedale Santo Spirito, Rome, Italy
[f] Diagnostic Imaging and Interventional Radiology Unit, Policlinico Casilino, Rome, Italy
[g] Cardiology Unit, Careggi Hospital, Florence, Italy

ARTICLE INFO

Keywords:
Cardiac amyloidosis
Cardiovascular magnetic resonance (CMR)
ECG
Echocardiogram
Extracellular volume (ECV)

ABSTRACT

Background: Cardiac amyloidosis (CA) is an infiltrative cardiomyopathy associated with adverse outcomes. Quantification of myocardial amyloid burden is essential for risk stratification. Although cardiac magnetic resonance (CMR)-derived extracellular volume (ECV) is the reference standard for non-invasive assessment, its use is limited by cost and availability. Therefore, simple and widely accessible tools to estimate amyloid burden are needed. This study aimed to evaluate whether a novel integrated echocardiographic–electrocardiographic (echo–ECG) index, based on the ratio of maximum septal thickness (MST) to QRS voltage in lead I and/or aVR, correlates with CMR-derived ECV in patients with CA.

Methods: We retrospectively analysed 138 consecutive patients with transthyretin or light-chain CA who underwent CMR at four Italian referral centres. MST/QRS ratios (MST/QRS I, MST/QRS aVR, and MST/(QRS I + aVR)) were calculated using echocardiography and standard 12-lead ECG.

Results: On multivariable linear regression with ECV as a continuous variable, the integrated echo–ECG indices were independently associated with ECV (all $p < 0.001$); lower QRS voltages in leads I and aVR were also independently associated with higher ECV (both $p < 0.01$), whereas total QRS voltage was not. In a secondary analysis dichotomising ECV at the cohort median (47%), the integrated echo–ECG indices showed moderate discrimination for higher ECV (AUC 0.71–0.73).

Conclusions: MST-to-QRS voltage ratios in leads I and/or aVR are simple and widely accessible markers that correlate with myocardial amyloid burden and may support non-invasive assessment of disease severity in CA.

1. Introduction

Cardiac amyloidosis (CA) is a systemic infiltrative disorder with substantial morbidity and mortality. The extent of myocardial amyloid deposition is a major prognostic determinant, with higher burden portending worse outcomes [1–3]. Disease-modifying therapies that can stabilize or reverse cardiac infiltration have further emphasized the need to accurately quantify amyloid burden [4–7].

Among non-invasive imaging modalities, cardiac magnetic resonance (CMR)-derived extracellular volume (ECV) is the most sensitive

* Corresponding author at: Cardiology Unit, Department of Clinical and Molecular Medicine, Sant'Andrea University Hospital, Sapienza University of Rome, Via di Grottarossa 1035, 00189 Rome, Italy.
E-mail address: matteo.sclafani@uniroma1.it (M. Sclafani).
[1] Contributed equally.

https://doi.org/10.1016/j.ijcard.2026.134670
Received 20 April 2026; Received in revised form 21 June 2026; Accepted 3 July 2026
Available online 14 July 2026

validated parameter for quantifying amyloid burden [8]. ECV has demonstrated superior reliability for monitoring disease progression compared with traditional markers (natriuretic peptides, high-sensitivity troponin T, NYHA class, Perugini grade, and echocardiographic parameters) [3,9]. However, CMR is costly, time-consuming, and not universally available, limiting its use in clinical practice.

Electrocardiography (ECG) and echocardiography are widely available, non-invasive tools routinely used in CA and may provide indirect markers of myocardial infiltration. Typical ECG findings include low QRS voltages, pseudoinfarct patterns, and conduction abnormalities, which usually occur in more advanced stages of disease [10,11].

There is therefore a need for simple, accessible parameters that reflect amyloid burden and can be implemented in routine clinical practice.

Lower QRS voltages correlate with higher amyloid burden and ECV [12], while an increased left ventricular mass-to-QRS voltage ratio is associated with worse prognosis [13]. Among ECG leads, QRS voltage in leads I (QRS I) and aVR (QRS aVR) appears particularly sensitive for early detection of CA [14,15]. Based on this evidence, we investigated a novel integrated echocardiographic–ECG index combining maximum septal thickness (MST), as a surrogate of left ventricular mass, with QRS amplitude in lead I and/or aVR.

The aim of this study was to assess whether the MST-to-QRS amplitude ratios (MST/QRS I, MST/QRS aVR, and MST/(QRS I + aVR)) correlate with CMR-derived ECV.

2. Methods

2.1. Study population

We retrospectively analysed 138 consecutive patients with transthyretin (ATTR) or immunoglobulin light-chain (AL) CA who underwent CMR at four Italian centers (Rome, Sant'Andrea University Hospital; Florence, Careggi University Hospital; Rome, Policlinico Casilino Hospital; Rome, Madre Giuseppina Vannini Hospital) between January 1, 2012, and December 31, 2023. Ethics approval was obtained at each site in accordance with local institutional requirements.

The diagnosis of CA was established according to contemporary guidelines and recommendations. Before 2016, ATTR CA was diagnosed based on the presence of heart failure symptoms with characteristic echocardiographic findings and histological confirmation of ATTR amyloid deposits on endomyocardial or extracardiac biopsy [16]. After 2016, diagnosis followed the Gillmore algorithm [17]. AL amyloidosis was confirmed by biopsy of abdominal fat or an involved organ, with amyloid typing by immunohistochemistry, immunoelectron microscopy, or proteomics [18].

Clinical data, ECG, echocardiographic measurements, and laboratory parameters were collected at the visit closest to CMR.

2.2. Cardiac magnetic resonance (CMR)

All patients underwent CMR on 1.5 T scanners (Siemens Aera, Siemens Sola, and Philips) using standardized protocols. Cine images were acquired with steady-state free precession sequences to assess biventricular volumes, mass, and function. Native and post-contrast T1 mapping (MOLLI or shMOLLI) were performed for extracellular volume (ECV) quantification, using regions of interest placed in the interventricular septum and blood pool (Fig. 1).

ECV was calculated from native and post-contrast T1 values, acquired before and 15 min after administration of 0.1 mmol/kg of a gadolinium-based contrast agent, and corrected for haematocrit measured on the day of the scan, according to established methods [19], validated for multicentre reproducibility across scanners and sequences [20].

Patients with metallic cardiovascular implants were excluded due to off-resonance artifacts affecting T1 measurements [21]. All CMR

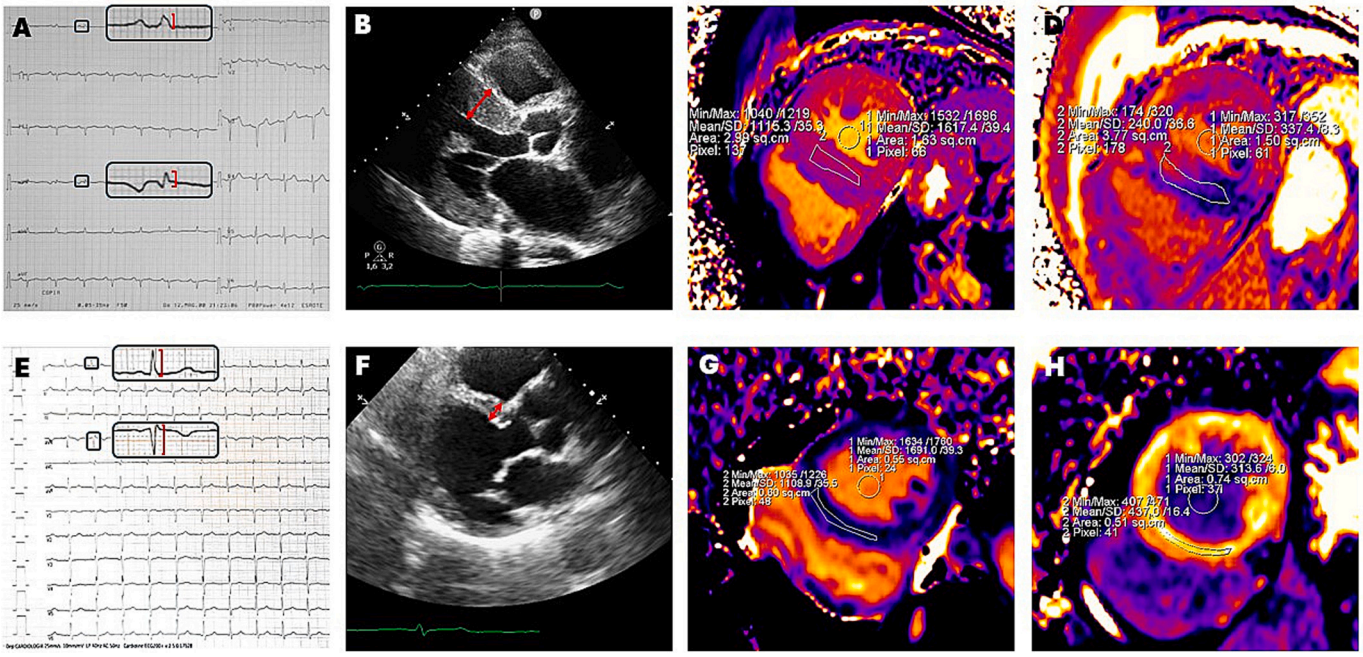

Fig. 1. Quantification of echo-ECG indices and extracellular volume (ECV) in two representative patients.
Panels A–D: Example of a patient with high myocardial amyloid burden (ECV 78%).
(A) Twelve-lead ECG showing markedly reduced QRS voltages in lead I (~0.20 mV) and lead aVR (~0.25 mV). (B) Parasternal long-axis echocardiographic view demonstrating increased maximum septal thickness (MST) of 19 mm. (C—D) Native and post-contrast T1-mapping images with septal and blood-pool regions of interest used to calculate ECV. Derived indices in this patient were markedly elevated: MST/QRS $I = 95$, MST/QRS aVR = 76, and MST/(QRS I + aVR) = 42.
Panels E–H: Example of a patient with lower myocardial amyloid burden (ECV 30%). (E) ECG showing higher QRS voltages in lead I (~0.40 mV) and lead aVR (~0.65 mV). (F) Echocardiographic assessment showing non-hypertrophic septal thickness (10 mm). (G–H) Corresponding native and post-contrast T1-mapping images for ECV quantification. In this patient, MST-to-QRS ratios were substantially lower: MST/QRS $I = 25$, MST/QRS aVR = 15, and MST/(QRS I + aVR) = 10.

analyses were performed by experienced operators using dedicated software. Additional details are provided in the **Supplementary Methods**.

2.3. Echocardiography

Echocardiography was performed using standard parasternal and apical views. Pulsed-wave and tissue Doppler imaging were used to assess diastolic function, graded according to guidelines [22].

Maximum septal thickness (MST) was measured by 2D echocardiography from the optimal acoustic window, with M-mode confirmation when feasible. Additional details are provided in the **Supplementary Methods**.

2.4. Electrocardiography

A standard 12-lead surface ECG (10 mm/mV, 25 mm/s) was obtained within three months of CMR. QRS voltages were measured manually by experienced cardiologists. QRS amplitude in leads I and aVR was measured as the peak-to-peak excursion of the QRS complex (the vertical distance between the tallest positive and deepest negative deflection), expressed as a positive value (Fig. 1). Patients with paced QRS complexes were excluded from the QRS voltage analysis.

2.5. Statistical analysis

Normality of data distribution was assessed by visual inspection and the Kolmogorov–Smirnov test. Continuous variables are presented as mean ± standard deviation (SD) for normally distributed data, or as median with interquartile range (IQR) for skewed data. Group comparisons were performed using the unpaired Student's *t*-test for normally distributed data and the Mann–Whitney *U* test for non-normally distributed data. Categorical variables were compared using the chi-square or Fisher's exact test, as appropriate.

Intra- and inter-observer reproducibility was assessed in a randomly selected subset of 31 patients. The echo-ECG indices (MST/QRS I, MST/QRS aVR) were independently re-measured by a second operator blinded to clinical data and to the original values (inter-observer), and by the original operator after an interval of ≥2 weeks (intra-observer). Agreement was quantified with the intraclass correlation coefficient (two-way random-effects model, absolute agreement, single measures) and Bland–Altman analysis.

ECV was analysed primarily as a continuous variable. For descriptive purposes only, patients were additionally stratified into two subgroups according to the cohort median ECV (47%). Associations between ECV and electrocardiographic or integrated echocardiographic-electrocardiographic (echo-ECG) parameters were assessed using multivariable linear regression adjusted for age, sex, amyloidosis subtype, left ventricular ejection fraction (LVEF), and cardiac rhythm. To assess whether the integrated echo-ECG indices provided incremental value over the isolated QRS voltages or MST alone, we performed hierarchical multivariable linear regression with ECV as the dependent variable. In separate models, a single isolated predictor (the QRS voltage in the relevant lead, or MST) was entered first with age and sex, and the corresponding integrated index added in a second block. Model improvement was assessed by the change in R^2 (ΔR^2) and its statistical significance (p for R^2 change); a significant ΔR^2 ($p < 0.05$) indicated incremental explanatory value of the integrated parameter beyond the isolated predictor. To verify that the associations were not driven by temporal discordance or amyloidosis subtype, we repeated the analysis in patients whose CMR and cardiology visit were within one month (adjusted for age, sex, and type) and, separately, in ATTR and AL patients (adjusted for age and sex).As a secondary, exploratory analysis, receiver operating characteristic (ROC) curves assessed the performance of individual and combined parameters in identifying patients with elevated ECV (cohort median, >47%). Optimal cutoffs were derived using the Youden index. Comparisons between ROC curves were performed using the DeLong test in MedCalc (version 23.3.7; MedCalc Software, Ostend, Belgium). All other analyses were conducted using SPSS Statistics (version 31.0; IBM Corp., Armonk, NY, USA). A two-tailed p value <0.05 was considered statistically significant.

3. Results

3.1. Study population

Among the 138 patients with confirmed CA who underwent CMR, 41 were excluded for missing ECV or absence of an ECG within 3 months of CMR, yielding a final cohort of 97 patients. Included and excluded patients did not differ in the principal markers of disease severity (Supplementary Table S1).

Patients were stratified according to the median ECV value into Group 1 (<47%; $n = 48$) and Group 2 (≥47%; $n = 49$).

3.2. Demographic and clinical characteristics

Baseline characteristics are summarized in Table 1. ATTR accounted for 70% of cases and AL for 30%. Mean age was 71.9 ± 10.1 years, and 73% were male. Median NYHA class was II (I–II), NT-proBNP 1976 pg/mL (615–3791) and NAC stage (ATTR only)1 (1–2).

Age and amyloidosis subtype did not differ between groups. Patients in Group 2 (higher ECV) were more frequently male and exhibited higher NT-proBNP levels, lower eGFR, more advanced NYHA class, and higher NAC stage compared with Group 1 (Table 1).

3.3. Cardiac magnetic resonance (CMR)

CMR was performed at a median of 4.9 months from the first formal diagnosis of CA (IQR: −3 to +7 months); negative values indicate that CMR preceded the formal diagnosis. Group 2 showed significantly higher indexed LV mass and lower LVEF than Group 1 (Table 1).

3.4. Echocardiography

Echocardiography was available for 96 patients; one patient in Group 2 had no echocardiogram at the visit closest to CMR.

The visit providing the ECG and echocardiogram was performed a median of −12 days relative to CMR (IQR −90 to 28; negative values indicate the visit preceded CMR), with no difference between the lower- and higher-ECV groups (median 10 [IQR −90 to 43] vs −44 [IQR −88 to 27] days; $p = 0.61$).

Compared with Group 1, Group 2 had higher MST, LV mass, and posterior wall thickness (PWT), larger left atrial volume index (LAVI), more advanced diastolic dysfunction, and lower TAPSE (Table 1).

3.5. Electrocardiography (ECG)

One patient in Group 2 was excluded from the QRS voltage analysis because of a pacemaker implanted between CMR and ECG.

At ECG acquisition, 76% of patients were in sinus rhythm and 24% in atrial fibrillation. Mean PR interval, QRS duration, QTc, QRS amplitudes in leads I and aVR, and total QRS voltage are reported in Table 1.

Groups did not differ in QRS duration, QTc interval, pseudoinfarct prevalence (all $p > 0.05$). Group 2 had longer PR interval ($p = 0.03$) and more atrial fibrillation (35% vs. 10%; $p = 0.007$). QRS amplitude in lead I was significantly lower in Group 2 (0.44 ± 0.21 vs. 0.57 ± 0.27 mV; $p = 0.02$), with a non-significant trend in lead aVR ($p = 0.06$). Total QRS voltage did not differ significantly ($p = 0.82$).

3.6. Integrated echo-ECG indices

Patients in Group 2 demonstrated significantly higher values of all

Table 1
Baseline characteristics of the patients.

Characteristic	Total	Lower ECV (< 47%)	Higher ECV (≥ 47%)	*P*-value
	N = 97	N = 48	N = 49	
Demographic and clinical characteristics				
Age (years)	71.9 ± 10.1	70.0 ± 10.4	73.8 ± 9.5	0.07
Male sex - n (%)	71 (73%)	30 (63%)	41 (84%)	**0.02**
ATTR - n/N (%)	65/93 (70%)	29/46 (63%)	36/47 (77%)	0.18
AL - n/N (%)	28/93 (30%)	17/46 (37%)	11/47 (23%)	0.18
BMI (kg/m^2)	25.0 ± 4.3	24.5 ± 4.1	25.5 ± 4.5	0.25
NYHA class	2 (1–2)	1.5 (1–2)	2 (1–2)	**0.04**
eGFR (mL/min) [N]	72.6 ± 28.0 [86]	86.6 ± 33.9 [44]	62.2 ± 17.8 [42]	**0.05**
NTproBNP (pg/ml) [N]	1976 (615–3791) [73]	615 (259–1427) [34]	3034 (1412–5890) [39]	**< 0.001**
NAC stage * [N]	1 (1–2) [57]	1 (1–1) [31]	1 (1–2) [26]	**0.005**
CMR characteristics				
LVEDVi (mL/m2)	77.9 ± 21.2	71.4 ± 19.8	84.4 ± 20.8	**0.002**
LVESVi (mL/m2)	37.6 ± 18.5	31.0 ± 16.7	44.2 ± 18.0	**< 0.001**
LVSVi (mL/m2)	39.9 ± 9.6	40.2 ± 9.8	39.6 ± 9.4	0.76
LV mass index (g/m2)	99.6 ± 35.8	88.9 ± 29.3	110.3 ± 38.7	**0.003**
LVEF (%)	53.3 ± 13.3	58.4 ± 13.3	48.4 ± 11.5	**< 0.001**
ECV (%)	46.5 ± 11.3	38.0 ± 6.2	55.0 ± 8.6	**< 0.001**
Echocardiographic characteristics				
MST (mm) [N]	15.1 ± 2.9 [96]	14.0 ± 2.9 [48]	16.3 ± 2.5 [48]	**< 0.001**
LVEDD (mm) [N]	44.0 ± 6.2 [96]	42.7 ± 6.4 [48]	45.4 ± 5.7 [48]	**0.03**
PWT (mm) [N]	13.6 ± 2.8 [96]	12.3 ± 2.5 [48]	15.0 ± 2.4 [48]	**< 0.001**
LAVi (mL/m2) [N]	41.5 ± 16.2 [79]	36.3 ± 13.0 [35]	45.6 ± 17.4 [44]	**0.01**
Diastolic dysfunction grade [N]	2 (1–3) [82]	1 (1–2) [41]	3 (2–3) [41]	**< 0.001**
TAPSE (mm) [N]	19.6 ± 4.5 [87]	20.7 ± 4.2 [43]	18.4 ± 4.5 [44]	**0.02**
LV mass (g) [N]	247.0 ± 85.1 [96]	204.8 ± 74.1 [48]	289.1 ± 74.2 [48]	**< 0.001**
Electrocardiographic characteristics				
AF - n/N (%)	23/96 (24%)	5/48 (10%)	18/48 (38%)	**0.007**
PR interval (ms) [N]	195.2 ± 41.4 [77]	186.2 ± 37.7 [34]	206.6 ± 43.5 [43]	**0.03**
QRS interval (ms) [N]	107.6 ± 25.2 [96]	105.5 ± 24.0 [48]	109.7 ± 26.3 [48]	0.41
QTc duration (ms) [N]	439.6 ± 28.7 [96]	435.0 ± 28.9 [48]	444.1 ± 28.2 [48]	0.12
Pseudoinfarct pattern - n/N (%)	47/96 (49%)	22/48 (46%)	25/48 (52%)	0.69
QRS I (mV) [N]	0.50 ± 0.25 [96]	0.57 ± 0.27 [48]	0.44 ± 0.21 [48]	**0.02**
QRS aVR (mV) [N]	0.46 ± 0.19 [96]	0.50 ± 0.19 [48]	0.43 ± 0.18 [48]	0.06
Total QRS voltage (mV) [N]	10.4 ± 3.1 [96]	10.3 ± 3.3 [48]	10.4 ± 2.9 [48]	0.82
Integrated Echocardiographic - Electrocardiographic Indices				
MST/QRS I [N]	32.0 (23.2–42.9) [95]	26.1 (21.3–35.8) [48]	37.5 (32.0–47.6) [47]	**< 0.001**
MST/QRS aVR [N]	33.3 (25.0–46.8) [95]	30.5 (22.5–37.2) [48]	40.0 (31.3–54.2) [47]	**< 0.001**
MST/(QRS I + aVR) [N]	16.2 (12.0–23.2) [95]	14.0 (10.7–18.2) [48]	20.0 (15.6–24.6) [47]	**< 0.001**
LV mass/total QRS voltage [N]	25.0 ± 9.5 [95]	20.7 ± 6.8 [48]	29.4 ± 9.9 [47]	**< 0.001**

Data are summarized as mean ± SD where normally distributed and median (IQR) where non-normally distributed.

ATTR: transthyretin-related cardiac amyloidosis. AL: immunoglobulin light chain- related cardiac amyloidosis. NYHA: New York Heart Association. eGFR: estimated glomerular filtration rate. NTproBNP: N-terminal pro B-type natriuretic peptide. LVEDVi: indexed left ventricular end-diastolic volume. LVESVi: indexed left ventricular end-systolic volume. LVSVi: indexed left ventricular stroke volume. LVEF: left ventricular ejection fraction. ECV: extracellular volume. MST: maximum septum thickness. LVEDD: left ventricular end-diastolic diameter. PWT: Posterior wall thickness. LAVi: Indexed left atrial volume. TAPSE: tricuspid annular plane systolic excursion. AF: atrial fibrillation; HR: heart rate. QRS I: QRS voltage in lead I. QRS aVR: QRS voltage in lead aVR. MST/QRS I: Maximum septal thickness to QRS voltage in lead I ratio. MST/QRS aVR: Maximum septal thickness to QRS voltage in lead aVR ratio. MST/(QRS I + aVR): Maximum septal thickness to the sum of QRS voltage in lead I and QRS voltage in lead aVR ratio.

* NAC stage measured only in ATTR patients.

three integrated echo-ECG indices and of the LV mass to total QRS voltage ratio than Group 1 (Table 1).

Findings were consistent in the sensitivity analysis restricted to patients with ATTR and AL CA (Supplementary Table S2).

3.7. Inter-observer and Intra-observer Reproducibility of Integrated Echo-ECG Indices

Reproducibility was high for all three indices. Inter-observer ICCs ranged from 0.92 to 0.99 and intra-observer ICCs from 0.91 to 0.99, with mean bias close to zero. On Bland–Altman analysis, no significant systematic inter- or intra-observer bias was observed for any index (Supplementary Table S3 and Supplementary Fig. S1 and S2).

3.8. Multivariable linear regression analysis

In our primary analysis ($n = 95$), with ECV as a continuous variable in the multivariable model, the integrated echo–ECG indices (MST/QRS I, MST/QRS aVR, and MST/(QRS I + aVR)) were all independently and positively associated with ECV (all $p < 0.001$; Table 2, Fig. 2), with a 0.21% (95% CI 0.12–0.30), 0.18% (95% CI 0.08–0.29), and 0.68% (95% CI 0.43–0.93) increase in ECV per one-unit increment in the respective

Table 2
Univariable and Multivariable Linear Regression Analysis of ECV.

Variables	Univariable		Multivariable	
	Unadjusted β (95% CI)	p-value	Adjusted β (95% CI)	p-value
MST/QRS I	0.19 (0.11 to 0.27)	**< 0.001**	0.21 (0.12 to 0.30)	**< 0.001**
MST/QRS aVR	0.17 (0.07 to 0.28)	**0.002**	0.18 (0.08 to 0.29)	**< 0.001**
MST/(QRS I + aVR)	0.63 (0.38 to 0.88)	**< 0.001**	0.68 (0.43 to 0.93)	**< 0.001**
QRS I	−16.6 (−25.3 to −7.9)	**< 0.001**	−18.9 (−26.5 to −11.3)	**< 0.001**
QRS aVR	−14.5 (−26.3 to −2.6)	**0.02**	−17.4 (−28.5 to −6.4)	**0.002**
PR interval	0.04 (−0.02 to 0.1)	0.19	0.03 (−0.04 to 0.1)	0.35
QRS duration	0.02 (−0.07 to 0.11)	0.61	−0.09 (−0.20 to 0.02)	0.10
Total QRS voltage	−0.17 (−0.92 to 0.58)	0.65	−0.40 (−1.20 to 0.40)	0.32

Multivariable models adjusted for age, sex, amyloidosis subtype (ATTR vs AL), left ventricular ejection fraction (LVEF), and cardiac rhythm (sinus rhythm vs atrial fibrillation). Integrated echo–ECG indices, $n = 95$; QRS I, QRS aVR, QRS duration and total QRS voltage, $n = 96$; PR interval, $n = 77$. MST/QRS I: Maximum septal thickness to QRS voltage in lead I ratio. MST/QRS aVR: Maximum septal thickness to QRS voltage in lead aVR ratio. MST/(QRS I + aVR): Maximum septal thickness to the sum of QRS voltage in lead I and QRS voltage in lead aVR ratio. QRS I: QRS voltage in lead I. QRS aVR: QRS voltage in lead aVR.

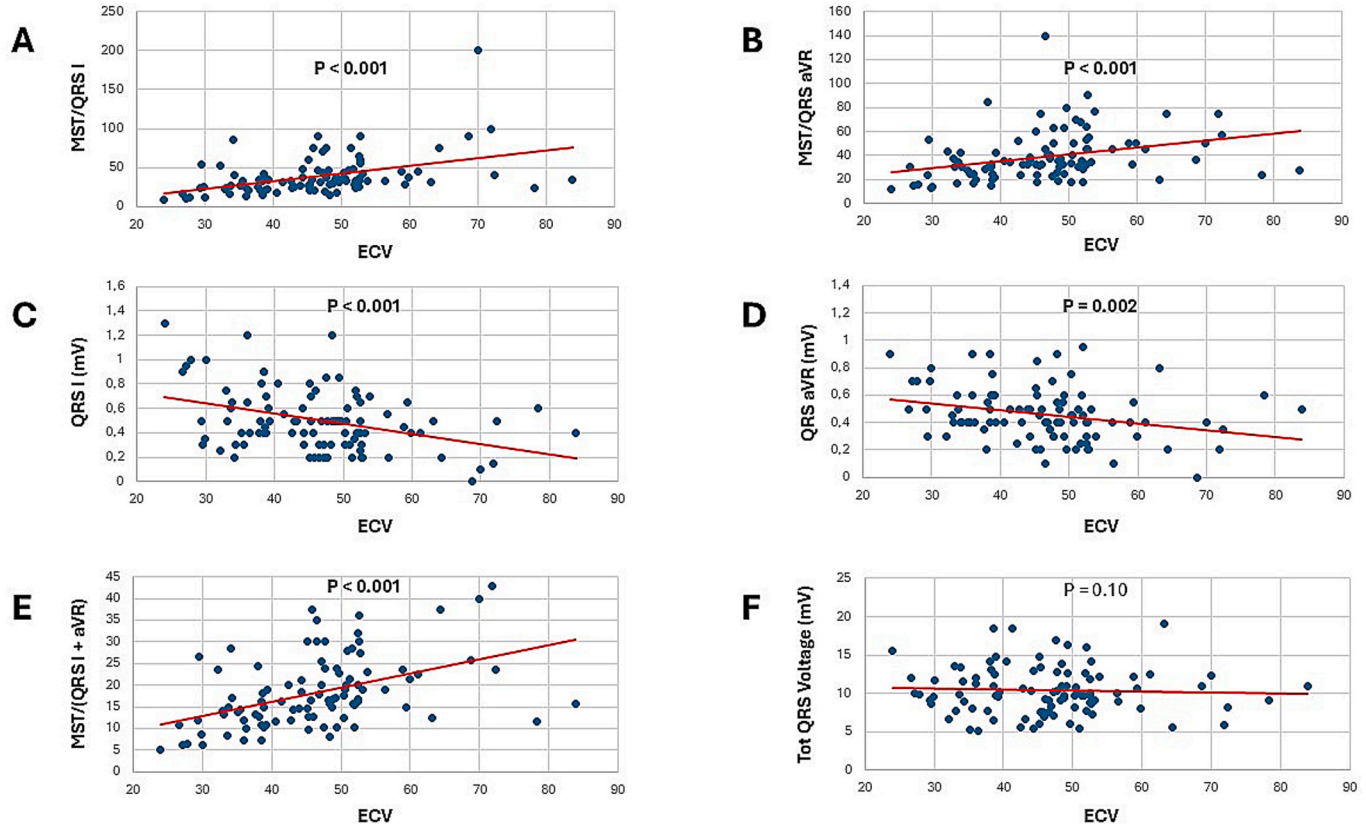

Fig. 2. Correlation between CMR-derived ECV and electrocardiographic/echocardiographic parameters in patients with cardiac amyloidosis.
Panels A–B: positive correlations between ECV and integrated echocardiographic–electrocardiographic ratios (MST/QRS I and MST/QRS aVR) (n = 95). Panel E: similar positive relationship for the combined MST/(QRS I + aVR) ratio (n = 95). Panels C–D: inverse correlations between ECV and QRS voltages in leads I and aVR, respectively (n = 96). Panel F: no significant association between ECV and total QRS voltage across all 12 leads (n = 96). Regression lines with 95% confidence intervals are shown; p values refer to multivariable linear regression analyses adjusted for age, sex, amyloidosis type (ATTR vs AL), left ventricular ejection fraction (LVEF), and cardiac rhythm (sinus rhythm vs atrial fibrillation).

index.

Among ECG-derived parameters, lower QRS voltages in leads I and aVR were independently associated with higher ECV (all $p < 0.05$), corresponding to an ECV increase of 18.9% for each 1-mV decrease in QRS I (95% CI −26.5 to −11.3, $p < 0.001$) and 17.4% for each 1-mV decrease in QRS aVR (95% CI −28.5 to −6.4, $p = 0.002$). Total QRS voltage, PR interval, and QRS duration were not significantly associated with ECV (all $p > 0.05$).

In the sensitivity analysis restricted to patients with a CMR-to-visit interval ≤ 1 month ($n = 42$), all three integrated echo–ECG indices remained independently associated with ECV (Supplementary Table S4). In the subgroup analyses by CA subtype, the indices remained independently associated with ECV in ATTR ($n = 63$); in AL ($n = 28$), the association remained significant for MST/QRS I and MST/(QRS I + aVR) but not for MST/QRS aVR (Supplementary Table S2). Adding body mass index to the primary model did not affect these associations (Supplementary Table S5).

3.9. Comparison of the integrated indices with isolated QRS voltages and MST

We next examined whether the integrated echo–ECG indices added explanatory value beyond their isolated components. Adding MST/QRS I and MST/QRS aVR to a model containing the corresponding isolated voltage (lead I and aVR, respectively) significantly increased the explained variance in ECV ($\Delta R^2 = 0.06$, $p = 0.011$ and $\Delta R^2 = 0.04$, $p = 0.04$, respectively), as did adding MST/(QRS I + aVR) to a model containing the voltages in both leads ($\Delta R^2 = 0.07$, $p = 0.003$). Similarly, adding MST/QRS I and MST/(QRS I + aVR) to a model including MST significantly increased the explained variance in ECV ($\Delta R^2 = 0.11$, $p < 0.001$ and $\Delta R^2 = 0.10$, $p < 0.001$, respectively), whereas MST/QRS aVR did not reach statistical significance ($\Delta R^2 = 0.03$, $p = 0.068$).

3.10. Diagnostic performance of electrocardiographic and integrated echo–ECG indices

The integrated echo–ECG indices demonstrated moderate discrimination for elevated ECV: MST/QRS I, MST/QRS aVR, and MST/(QRS I + aVR) achieved areas under the curve (AUC) values of 0.73 (95% CI 0.62–0.83, $p < 0.001$), 0.71 (95% CI 0.60–0.81, $p < 0.001$), and 0.73 (95% CI 0.62–0.83, $p < 0.001$), respectively (Supplementary Table S6, Supplementary Fig. S3).

Optimal cutoff values were 27.6 for MST/QRS I (sensitivity 87%, specificity 58%), 32.6 for MST/QRS aVR (sensitivity 73%, specificity 67%), and 14.9 for MST/(QRS I + aVR) (sensitivity 85%, specificity 63%).

In contrast, isolated ECG voltages showed modest discrimination. QRS amplitudes in leads I and aVR yielded AUCs of 0.63 (95% CI 0.52–0.74, $p = 0.02$) and 0.63 (95% CI 0.51–0.74, $p = 0.03$), respectively, while total QRS voltage did not discriminate (AUC 0.52, 95% CI 0.40–0.63, $p = 0.77$).

On comparative ROC analysis, MST/QRS I outperformed QRS I alone (AUC 0.73 vs. 0.63; ΔAUC = 0.11, 95% CI 0.05–0.17; $p < 0.001$, DeLong test), and MST/QRS aVR outperformed QRS aVR (AUC 0.71 vs. 0.63; ΔAUC = 0.08, 95% CI 0.03–0.14; $p = 0.002$, DeLong test).

The LV mass-to-total QRS voltage ratio showed moderate

discrimination for elevated ECV (AUC 0.77, 95% CI 0.67–0.85), comparable to that of the integrated echo–ECG indices, with no significant pairwise differences on DeLong testing (vs MST/QRS I, ΔAUC 0.04, 95% CI −0.08 to 0.16, $p = 0.48$; vs MST/QRS aVR, ΔAUC 0.06, 95% CI −0.04 to 0.17, $p = 0.23$; vs MST/(QRS I + aVR), ΔAUC 0.04, 95% CI −0.07 to 0.15, $p = 0.75$) (Supplementary Fig. S4).

4. Discussion

This multicentre study evaluated novel integrated echo–ECG indices against myocardial ECV in patients with CA.

The main findings are as follows:

1. QRS voltages in leads I and aVR were inversely associated with amyloid burden, whereas the summed QRS voltage across all 12 leads was not.
2. All three integrated echo–ECG indices (MST/QRS I, MST/QRS aVR, and MST/(QRS I + aVR) ratios) were independently and positively associated with ECV.
3. All three integrated echo–ECG indices provided significant incremental explanatory value over the isolated ECG voltages and demonstrated superior discrimination in identifying patients with higher ECV.
4. MST/QRS I and MST/(QRS I + aVR) provided significant incremental value beyond MST alone, and all three indices showed discrimination similar to the LV mass-to-total QRS voltage ratio.

4.1. Clinical relevance of ECV and disease severity

CMR-derived ECV is a robust and validated marker of amyloid burden, reflecting interstitial expansion from amyloid deposition [1,3]. Higher ECV values have consistently been associated with more advanced myocardial involvement, impaired cardiac function, and adverse clinical outcomes in both AL and ATTR amyloidosis [1,23–26]. Proposed risk thresholds are approximately 44% for AL and 40% for ATTR [3,24]. Because clinically meaningful ECV thresholds differ by amyloid subtype, we analysed ECV primarily as a continuous variable; the cohort median (47%) was used only for descriptive comparison and for a secondary, exploratory discrimination analysis, and is not proposed as a clinical threshold.

Consistent with prior evidence, patients with higher ECV values in our cohort exhibited features of more advanced disease: worse functional class, higher NT-proBNP levels, reduced LVEF, and more severe diastolic dysfunction. These findings further support the role of ECV as a key marker for disease severity [4,27].

4.2. QRS voltage in leads I and aVR as markers of amyloid burden

Low QRS voltage is a well-recognised feature of CA and reflects the combined effects of amyloid infiltration, myocyte loss, and electrical insulation [28–31]. Reduced QRS voltage has been associated with myocardial amyloid burden assessed by histology or CMR [10,12]. More recently, QRS voltage in leads I and aVR has been suggested to be more sensitive than traditional ECG criteria in detecting amyloid involvement [14,15].

In the present multicentre study, we specifically evaluated QRS voltages in leads I and aVR and found a significant inverse association with amyloid burden, whereas summed QRS voltage across all 12 leads was not associated.

The greater sensitivity of leads I and aVR, likely reflects their anatomical orientation along the heart's principal electrical axis (albeit in opposite directions), rendering them particularly sensitive to attenuation and dispersion of the depolarization vector caused by amyloid infiltration. The lack of association between global QRS voltage and amyloid burden, in contrast with some previous reports, may reflect the lower disease severity of our cohort (median ECV 47%) [25,32,33]. In earlier stages, subtle voltage reductions may be detectable only in the most sensitive leads (i.e., I and aVR), whereas affecting global voltage may require more extensive deposition.

Low QRS voltage is not specific to amyloid and may be influenced by extracardiac factors such as obesity. However, body mass index was similar between ECV groups (Table 1), and its addition to the model did not alter the associations (Supplementary Table S5), making obesity an unlikely explanation.

4.3. Integrated echo–ECG indices: a simple surrogate of amyloid burden

The discordance between increased myocardial wall thickness and reduced QRS voltage is a hallmark of CA and reflects wall thickening driven by extracellular amyloid deposition rather than true myocyte hypertrophy [30,34–37].

Building on this concept, we evaluated a novel integrated index combining MST with QRS voltage in leads I and aVR. The MST/QRS ratios were highly reproducible and independently associated with ECV, outperforming the isolated voltages both as correlates and in discriminating elevated ECV. They also provided incremental value beyond MST alone, with discriminative performance comparable to the established LV mass-to-total QRS voltage ratio. From a practical standpoint, this approach offers several advantages. Both ECG and echocardiography are universally available, inexpensive, and routinely performed in CA. The proposed index relies on simple and reproducible measurements easily applicable in daily clinical practice.

Importantly, these indices may represent a pragmatic surrogate of myocardial amyloid burden. Further longitudinal studies are needed to assess their value for monitoring over time, treatment-response, and prognosis.

4.4. Clinical implications

Accurate quantification of amyloid burden is increasingly relevant in the era of disease-modifying therapies. While CMR-derived ECV remains the reference standard, its limited availability restricts widespread use. In this context, integrated echo–ECG indices may complement current clinical assessment by providing a simple, accessible, and immediately obtainable estimate of amyloid burden, which could be particularly valuable in non-specialist centres. The use of these indices for serial assessment and for guiding clinical decisions over time remains hypothesis-generating and requires prospective longitudinal validation.

5. Limitations

Some limitations should be acknowledged. First, the retrospective design limits causal inference. Second, the cohort size was relatively modest, and our population predominantly consisted of patients with less advanced disease and lower amyloid burden, as defined by ECV, compared with other published cohorts [25,32,33]. This likely reflects the evolving clinical profile of contemporary CA populations, particularly those with ATTR, where earlier diagnosis and the wider availability of disease-modifying therapies have led to a shift toward milder phenotypes at presentation [38,39]. Third, the cohort comprised both ATTR and AL patients. Although amyloidosis type was included as a covariate and the indices generally remained associated with ECV within both subtypes (Supplementary Table S2), the proposed indices may not perform identically across subtypes, and subtype-specific validation in larger cohorts is required. Fourth, the study was not longitudinal, and therefore prognostic correlations could not be assessed. Replication of these findings in larger populations is warranted. In addition, different CMR scanners and protocols were used across centres; although such multicentre settings are reliable [20], this may have introduced minor variability in ECV quantification. Finally, patients with cardiac implantable electronic devices were not eligible for CMR-based ECV

because of off-resonance artifacts on T1 mapping, an inherent limitation of ECV-based studies that may under-represent individuals with advanced conduction disease. Reassuringly, excluded patients did not differ from included patients in conduction parameters, atrial-fibrillation prevalence, or disease-severity markers (Supplementary Table S1).

6. Conclusions

A higher amyloid burden, as assessed by ECV, is associated with clinical features indicative of more advanced disease, consistent with the established prognostic value of ECV. QRS voltages in leads I and aVR reflect amyloid burden more closely than the sum of QRS amplitudes across all 12 leads. The ratio of maximum septal thickness to QRS voltage in lead I and/or aVR demonstrates a stronger association with amyloid burden than the isolated voltages and identifies patients with elevated ECV with moderate accuracy. These indices emerge as simple, accessible, and practical tools for estimating cardiac amyloid burden.

CRediT authorship contribution statement

Matteo Sclafani: Writing – review & editing, Writing – original draft, Methodology, Investigation, Formal analysis, Data curation, Conceptualization. **Luca Arcari:** Writing – review & editing, Supervision, Conceptualization. **Giacomo Tini:** Writing – review & editing, Supervision, Conceptualization. **Damiano Venturiello:** Validation. **Andrea Imperatrice:** Validation. **Alessandro Tropea:** Validation. **Elisa Fedele:** Validation. **Fabiana Romeo:** Validation. **Annamaria Martino:** Validation. **Domitilla Russo:** Validation. **Armando Fusco:** Validation. **Pietro Francia:** Writing – review & editing, Supervision. **Giovanni Camastra:** Validation. **Elisa Silvetti:** Validation. **Stefano Canestrelli:** Validation. **Leonardo Calò:** Validation. **Luca Cacciotti:** Validation. **Chiara Lanzillo:** Validation. **Francesco Cappelli:** Validation. **Beatrice Musumeci:** Writing – review & editing, Visualization, Validation, Supervision, Investigation, Conceptualization. **Emanuele Barbato:** Validation, Supervision.

Funding

This research did not receive any specific grant from funding agencies in the public, commercial, or not-for-profit sectors.

Declaration of competing interest

The authors declare that they have no known competing financial interests or personal relationships that could have appeared to influence the work reported in this paper.

Acknowledgements

All authors declare no competing interests. MS has been supported by a research grant provided by the DigicardiopaTh PhD program.

Appendix A. Supplementary data

Supplementary data to this article can be found online at https://doi.org/10.1016/j.ijcard.2026.134670.

Data availability

The data underlying this article cannot be shared publicly due to ethical and regulatory restrictions designed to protect the privacy of the individuals that participated in the study.

References

[1] S.M. Banypersad, M. Fontana, V. Maestrini, D.M. Sado, G. Captur, A. Petrie, et al., T1 mapping and survival in systemic light-chain amyloidosis, Eur. Heart J. 36 (2015) 244–251, https://doi.org/10.1093/eurheartj/ehu444.
[2] P. Garcia-Pavia, C. Rapezzi, Y. Adler, M. Arad, C. Basso, A. Brucato, et al., Diagnosis and treatment of cardiac amyloidosis: a position statement of the ESC working group on myocardial and pericardial diseases, Eur. Heart J. 42 (2021) 1554–1568, https://doi.org/10.1093/eurheartj/ehab072.
[3] A. Sheikh, A. Achten, A. Aimo, Y. Razvi, J. Mansell, M.U. Rauf, et al., Myocardial amyloid burden in transthyretin amyloidosis, J. Am. Coll. Cardiol. (25) (2025) S0735–S1097, https://doi.org/10.1016/j.jacc.2025.10.054.
[4] M. Fontana, A. Martinez-Naharro, L. Chacko, D. Rowczenio, J.A. Gilbertson, C. J. Whelan, et al., Reduction in CMR derived extracellular volume with Patisiran indicates cardiac amyloid regression, JACC Cardiovasc. Imaging 14 (2021) 189–199, https://doi.org/10.1016/j.jcmg.2020.07.043.
[5] A. Porcari, A. Masi, A. Martinez-Naharro, Y. Razvi, R. Patel, A. Ioannou, et al., Redefining cardiac involvement and targets of treatment in systemic immunoglobulin AL amyloidosis, JAMA Cardiol. 9 (2024) 982–989, https://doi.org/10.1001/jamacardio.2024.2555.
[6] F. Duca, M. Poledniczek, C. Kronberger, C. Binder, R. Rettl, L. Camuz-Ligios, et al., Serial extracellular volume quantification using cardiac magnetic resonance imaging in transthyretin amyloidosis patients treated with tafamidis, Eur. Radiol. 36 (2026) 172–181, https://doi.org/10.1007/s00330-025-11792-x.
[7] R.K. Patel, A. Ioannou, A. Sheikh, Y. Razvi, J. Mansell, A. Martinez-Naharro, et al., Transthyretin amyloid cardiomyopathy: natural history and treatment response assessed by cardiovascular magnetic resonance, Eur. Heart J. 46 (2025) 5049–5058, https://doi.org/10.1093/eurheartj/ehaf412.
[8] A. Pucci, A. Aimo, V. Musetti, A. Barison, G. Vergaro, D. Genovesi, et al., Amyloid deposits and fibrosis on left ventricular endomyocardial biopsy correlate with extracellular volume in cardiac amyloidosis, J. Am. Heart Assoc. 10 (2021) e020358, https://doi.org/10.1161/JAHA.120.020358.
[9] Y. Razvi, A. Porcari, D.F. Hutt, J. Lazari, A. Ioannou, R.K. Patel, et al., Uncertain clinical relevance of serial bone scintigraphy findings in treated transthyretin amyloid cardiomyopathy, JACC Cardiovasc. Imaging 18 (2025) 899–908, https://doi.org/10.1016/j.jcmg.2025.03.014.
[10] X. Guo, Z. Chen, K. Wan, R. Song, T. Yang, Y. Xu, Characteristics and Prognostic Value in Light-Chain Amyloidosis : A Comparison With Cardiac Magnetic Resonance Imaging 8, 2021, pp. 1–9, https://doi.org/10.3389/fcvm.2021.751422.
[11] A. Argirò, M. Zampieri, C. Mazzoni, C. Fumagalli, M. Baccini, A. Mattei, et al., Progression and Prognostic Significance of Electrocardiographic Findings in Patients with Cardiac Amyloidosis, 2025, pp. 809–818, https://doi.org/10.1002/ehf2.14684.
[12] F. Duca, R. Rettl, C. Kronberger, M. Poledniczek, C. Binder, D. Dalos, et al., Amyloid burden correlates with electrocardiographic findings in patients with cardiac amyloidosis-insights from histology and cardiac magnetic resonance imaging, J. Clin. Med. 13 (2024), https://doi.org/10.3390/jcm13020368.
[13] J.A. Slivnick, A.L. Wallner, A. Vallakati, V.T. Truong, W. Mazur, M.B. Elamin, et al., Indexed left ventricular mass to QRS voltage ratio is associated with heart failure hospitalizations in patients with cardiac amyloidosis, Int. J. Card. Imaging 37 (2021) 1043–1051, https://doi.org/10.1007/s10554-020-02059-1.
[14] J. Huang, S. Zhao, Z. Chen, S. Zhang, M. Lu, Contribution of electrocardiogram in the differentiation of cardiac amyloidosis and nonobstructive hypertrophic cardiomyopathy, Int. Heart J. 56 (2015) 522–526, https://doi.org/10.1536/ihj.15-005.
[15] A. Vereckei, G. Katona, G. Szénási, L.D. Vidács, D. Földeák, H. Takács, et al., Novel electrocardiographic criteria may render possible the more accurate recognition of cardiac amyloidosis, ESC Heart Fail. 11 (2024) 1030–1038, https://doi.org/10.1002/ehf2.14655.
[16] M.A. Gertz, M.D. Benson, P.J. Dyck, M. Grogan, T. Coelho, M. Cruz, et al., Diagnosis, prognosis, and therapy of transthyretin amyloidosis, J. Am. Coll. Cardiol. 66 (2015) 2451–2466, https://doi.org/10.1016/j.jacc.2015.09.075.
[17] J.D. Gillmore, M.S. Maurer, R.H. Falk, G. Merlini, T. Damy, A. Dispenzieri, et al., Heart failure nonbiopsy diagnosis of cardiac transthyretin amyloidosis, Circulation 133 (2016) 2404–2412, https://doi.org/10.1161/CIRCULATIONAHA.116.021612.
[18] F.L. Ruberg, R.K. Cheng, C. Ms, J.O. Clarke, L.M. Dember, R.E. Hershberger, et al., ACC Expert Consensus Decision Pathway on Comprehensive Multidisciplinary Care for the Patient With Cardiac Amyloidosis 81, 2023, https://doi.org/10.1016/j.jacc.2022.11.022.
[19] D.R. Messroghli, J.C. Moon, V.M. Ferreira, L. Grosse-wortmann, T. He, P. Kellman, et al., Clinical recommendations for cardiovascular magnetic resonance mapping of T1, T2, T2 * and extracellular volume : a consensus statement by the Society for Cardiovascular Magnetic Resonance (SCMR) endorsed by the European Association for Cardiovascular, J. Cardiovasc. Magn. Reson. 19 (2017) 1–24, https://doi.org/10.1186/s12968-017-0389-8.
[20] R.J. Everett, T.A. Treibel, M. Fukui, H. Lee, M. Rigolli, A. Singh, et al., Extracellular myocardial volume in patients with aortic stenosis, J. Am. Coll. Cardiol. 75 (2020) 304–316, https://doi.org/10.1016/j.jacc.2019.11.032.
[21] A.N. Bhuva, T.A. Treibel, A. Seraphim, P. Scully, K.D. Knott, J.B. Augusto, et al., Measurement of T1 mapping in patients with cardiac devices: off-resonance error extends beyond visual artifact but can be quantified and corrected, Front. Cardiovasc. Med. 8 (2021) 631366, https://doi.org/10.3389/fcvm.2021.631366.
[22] S.F. Nagueh, O.A. Smiseth, C.P. Appleton, B.F. Byrd, H. Dokainish, T. Edvardsen, et al., Recommendations for the evaluation of left ventricular diastolic function by echocardiography : an update from the American Society of Echocardiography and

the European Association of Cardiovascular Imaging, J. Am. Soc. Echocardiogr. 29 (2016) 277–314, https://doi.org/10.1016/j.echo.2016.01.011.
[23] T.C. Wong, K. Piehler, C.G. Meier, S.M. Testa, A.M. Klock, A.A. Aneizi, et al., Association between extracellular matrix expansion quantified by cardiovascular magnetic resonance and short-term mortality, Circulation 126 (2012) 1206–1216, https://doi.org/10.1161/CIRCULATIONAHA.111.089409.
[24] L. Lin, X. Li, J. Feng, K.-N. Shen, Z. Tian, J. Sun, et al., The prognostic value of T1 mapping and late gadolinium enhancement cardiovascular magnetic resonance imaging in patients with light chain amyloidosis, J. Cardiovasc. Magn. Reson. 20 (2018) 2, https://doi.org/10.1186/s12968-017-0419-6.
[25] A. Martinez-Naharro, T. Kotecha, K. Norrington, M. Boldrini, T. Rezk, C. Quarta, et al., Native T1 and extracellular volume in transthyretin amyloidosis, JACC Cardiovasc. Imaging 12 (2019) 810–819, https://doi.org/10.1016/j.jcmg.2018.02.006.
[26] T.D. Karamitsos, S.K. Piechnik, S.M. Banypersad, M. Fontana, N.B. Ntusi, V. M. Ferreira, et al., Noncontrast T1 mapping for the diagnosis of cardiac amyloidosis, JACC Cardiovasc. Imaging 6 (2014) 488–497, https://doi.org/10.1016/j.jcmg.2012.11.013.
[27] M. Fontana, S. Pica, P. Reant, A. Abdel-Gadir, T.A. Treibel, S.M. Banypersad, et al., Prognostic value of late gadolinium enhancement cardiovascular magnetic resonance in cardiac amyloidosis, Circulation 132 (2015) 1570–1579, https://doi.org/10.1161/CIRCULATIONAHA.115.016567.
[28] C. Rapezzi, G. Merlini, C.C. Quarta, L. Riva, S. Longhi, O. Leone, et al., Systemic cardiac amyloidoses disease profiles and clinical courses of the 3 main types, Circ. Cardiovasc. Imaging 120 (2009) 1203–1212, https://doi.org/10.1161/CIRCULATIONAHA.108.843334.
[29] A. Cipriani, L. De Michieli, A. Porcari, L. Licchelli, G. Sinigiani, G. Tini, et al., Low QRS voltages in cardiac amyloidosis: clinical correlates and prognostic value, JACC CardioOncol. 4 (2022) 458–470, https://doi.org/10.1016/j.jaccao.2022.08.007.
[30] J.E. Rahman, E.F. Helou, R. Gelzer-bell, R.E. Thompson, C. Kuo, E.R. Rodriguez, et al., Noninvasive diagnosis of biopsy-proven cardiac amyloidosis, J. Am. Coll. Cardiol. 43 (2004) 410–415, https://doi.org/10.1016/j.jacc.2003.08.043.
[31] T. Kotecha, A. Martinez-Naharro, T.A. Treibel, R. Francis, S. Nordin, A. Abdel-Gadir, et al., Myocardial edema and prognosis in amyloidosis, J. Am. Coll. Cardiol. 71 (2018) 2919–2931, https://doi.org/10.1016/j.jacc.2018.03.536.
[32] M. Boldrini, F. Cappelli, L. Chacko, M.A. Restrepo-Cordoba, A. Lopez-Sainz, A. Giannoni, et al., Multiparametric echocardiography scores for the diagnosis of cardiac amyloidosis, JACC Cardiovasc. Imaging 13 (2020) 909–920, https://doi.org/10.1016/j.jcmg.2019.10.011.
[33] J.A. Pan, M.J. Kerwin, M. Salerno, Native T1 mapping, extracellular volume mapping, and late gadolinium enhancement in cardiac amyloidosis, JACC Cardiovasc. Imaging 13 (2020) 1299–1310, https://doi.org/10.1016/j.jcmg.2020.03.010.
[34] J.D. Carroll, W.H. Gaasch, K.P. McAdam, Amyloid cardiomyopathy: characterization by a distinctive voltage/mass relation, Am. J. Cardiol. 49 (1982) 90270–90273, https://doi.org/10.1016/0002-9149(82)90270-3.
[35] Z. Cheng, L. Kang, Z. Tian, W. Chen, W. Guo, J. Xu, et al., Utility of combined indexes of electrocardiography and echocardiography in the diagnosis of biopsy proven primary cardiac amyloidosis, Ann. Noninvasive Electrocardiol. 16 (2011) 25–29, https://doi.org/10.1111/j.1542-474X.2010.00403.x.
[36] R.H. Falk, K.M. Alexander, R. Liao, S. Dorbala, AL (light-chain) cardiac amyloidosis, J. Am. Coll. Cardiol. 68 (2016) 1323–1341, https://doi.org/10.1016/j.jacc.2016.06.053.
[37] A. Martinez-Naharro, T.A. Treibel, A. Abdel-Gadir, H. Bulluck, G. Zumbo, D. S. Knight, et al., Magnetic resonance in transthyretin cardiac amyloidosis, J. Am. Coll. Cardiol. 70 (2017) 466–477, https://doi.org/10.1016/j.jacc.2017.05.053.
[38] A. Ioannou, R.K. Patel, Y. Razvi, A. Porcari, P. Massa, D. Knight, et al., Impact of earlier diagnosis in cardiac ATTR amyloidosis over the course of 20 years, Circulation 146 (2022) 1657–1670, https://doi.org/10.1161/CIRCULATIONAHA.122.060852.
[39] G. Tini, E. Cristiano, M. Zampieri, A. Ponziani, A. Porcari, M. Zanoletti, et al., Impact of the noninvasive diagnostic algorithm on clinical presentation and prognosis in cardiac amyloidosis, JACC. Adv. 3 (2024) 101232, https://doi.org/10.1016/j.jacadv.2024.101232.